Tellurite-filled hexa-circular-shaped PCF with highly nonlinearity, birefringent and near-zero dispersion profile for optical communications

Md. S. Hasan Sohag [a,b,*], K. H. Kabir [a]
[a]*Department of Electrical and Electronic Engineering, Islamic University of Technology, Board Bazar, Gazipur-1704, Dhaka, Bangladesh.*
[b]*Department of Electrical and Electronic Engineering, Bangladesh University of Business and Technology, Rupnagar, Mirpur-2, Dhaka-1216, Bangladesh.*

This manuscript focuses on devising a Tellurite-filled circular-timbered PCF that shows considerably highly birefringent and nonlinear characteristics. The impacts of numerous design parameters, such as birefringence (Br), nonlinear coefficients (NLC), confinement loss (CL), effective mode area (EMA), dispersion, numerical aperture (NA), etc. of the fiber are extensively inspected employing the commercially accessible and simulation-friendly COMSOL Software. Besides, the pertinent modal properties of the modeled fiber are rigorously characterized by operating the full-vector finite element method (FEM) with a perfectly matched layer (PML) boundary condition. The simulated findings affirm that the developed fiber exemplifies an ultra-high Br and NLC of 0.0924 and 18900 $W^{-1}Km^{-1}$ consecutively, at the operational wavelength of 1.55µm. Notably, the offered PCF also reveals a relatively lower CL, a negative-sloping dispersion and a higher EMA at the same wavelength. The pragmatic execution of the modeled fiber is expected to be doable applying the existing fabrication approaches and it can be applied in miscellaneous identical optical domains, namely polarization retention in long-distance communications, optical switching, sensor and laser layout, supercontinuum generation for frequency metrology and so forth.

(Received April 23, 2022; Accepted July 22, 2022)

Keywords: Photonic crystal fiber, Confinement loss, Nonlinearity, Dispersion, Birefringence, Effective mode area

1. Introduction

Photonic crystal fibers (PCFs) are a novel kind of optical fiber that depicts a much-upgraded and next-generational genre of ubiquitous and remarkably thriving technology. PCFs have risen to the top of the scientific priority list in recent years, attracting the interest of a growing number of researchers throughout the globe. Through their freedom from the constraints of traditional optical fibers, PCFs have ushered in an era of new potential prospects across a wide range of myriad domains of research and technology, irreversibly shattering many of the debilitated fundamentals of traditional fiber optics theory and practice in the process [1–5]. PCFs hold a plethora of special distinctive features that are quite challenging to accomplish in traditional fiber optics. To illustrate, the light-guiding mechanism in classical fibers is established upon two concentric domains with varying doping extents, namely core and clad; however, in PCFs, light is corralled inside a frequent and infinitesimal array of air holes, which is based on slight deviations in the refractive index (RI) and as a result, the clad remains substantially wavelength dependent [6]. Notably, thanks to this peculiar wavelength dependency, a variety of uncommon and tailorable optical features are possible in PCFs. This new technology, unlike the early stages of fiber optics, when just a handful number of fibers were accessible, allows for more flexibility in terms of light direction, manufacturing procedures, fiber materials and topologies. These extraordinary advancements enable them to demonstrate a wide variety of intriguing and

*Corresponding author: sabbirador2@gmail.com
https://doi.org/10.15251/JOR.2022.184.527

technologically boosting features that have been proved to outperform conventional technology in various ways [6–8].

PCFs can be tailored to meet the needs of a wide range of distinctive purposes, including being single-mode over an exceedingly wider wavelength extent [9], supporting more extensive or diminutive diameters in terms of mode-field distribution [10–11], meeting particular dispersion prerequisites [12], expanding or diminishing nonlinearity [13–14], as well as being highly birefringent, which results in enhanced polarization maintenance [15–16]. Because of the large disparity in RI between the core and clad precincts, PCFs offer substantially greater mode confinement and consequently, much larger nonlinear responses [13]. Additionally, the PCFs enable significantly more adjustable customization of the dispersion parameters [12, 17], which are imperative for numerous nonlinear utilization due to their high flexibility. Particularly, the ultra-high nonlinear and birefringent responses are two of the most pivotal traits of PCF. Highly birefringent PCF has a variety of exciting applications, including polarization retention in long-distance communications, optical sensor layout, etc. Similarly, highly nonlinear PCF serves notable purposes in optical switching layout, laser usage, supercontinuum generation for frequency metrology and so on [18–20]. Furthermore, PCFs have attracted considerable attention and applications in a variety of pertinent fields, including spectroscopy, sensors, tomography, metrology, lasers, biomedical imaging, telecommunications, etc., [18–23].

In recent years, a decent number of silica and tellurite based PCFs have been introduced for opening cutting-edge and new windows for prospective applications in a variety of pertinent disciplines of optics and photonics. In light of this, Wang et al. recently introduced a tellurite-based micro-structured core PCF to reach highly birefringent and nonlinear optical features. By optimizing the structural parameters, they consecutively delineated a NLC and Br of $1896\,W^{-1}Km^{-1}$ and 5.05×10^{-2} at the active wavelength of $1550\,nm$. In addition, the installment of 6 tiny slots in the PCF core, placed in a rectangular pattern, yielded a near elliptic core in their specified geometry [24]. Likewise, Liu et al. focused on designing an elliptical tellurite core-filled PCF to attain the above-alluded optical traits. Particularly, by fine-tuning the size and shape of the core, the Br can be increased up to the order of 7.57×10^{-2}, while the NLC can be boosted to as high as $188.39\,W^{-1}Km^{-1}$ at the useful wavelength of $1550\,nm$ [25]. Lately, Paul et al. reported on a modified square-patterned PCF to gain negative-sloping dispersion attributes for optical communication windows. Their silica-based architecture flaunted a nonlinear behavior of $74.68\,W^{-1}Km^{-1}$ at $1550\,nm$ wavelength [26]. Besides, most recently, another group of researchers documented two tellurite-filled PCFs, where the authors sequentially obtained a considerably high NLC and Br of $7333\,W^{-1}Km^{-1}$ and 5.85×10^{-2} at the active optical wavelength of $1550\,nm$ in their octa-spiral with octagonal PCF. Notably, their modeled fiber is comprised of perplexed geometrical architecture, which makes its fabrication procedures relatively challenging [27]. Further, in another research investigation, Ahmed et al. employed 2 sorts of air holes (elliptical and circular) in their modeled PCF architecture to investigate multiple optical traits. They successively managed to acquire NLC and Br up to the order of $23.46\,W^{-1}Km^{-1}$ and 2.2×10^{-3} at $1550\,nm$ wavelength [28].

It is obvious from the above-alluded literature review that plenty of exciting base materials have been practiced in recent years to fine-tune the modal attributes of PCFs, involving fused silica [20, 28–30], graphene [31–32], GaP [33–34], tellurite [24–25, 27], chalcogenide [38], Si_7N_3 [19], GaAs [35], ZBLAN [36], TOPAS [39–42], As_2S_3 and As_2S_5 [37], etc. Particularly, among the substances enumerated above, fused silica is regarded as the most continually operated base material. Nevertheless, when operated in this fashion, silica can only acquire comparatively minimal nonlinear and birefringent responses. Thus, in order to compensate for the inherent flaws of silica, a plethora of other suitable substances are often operated to obtain significantly higher Br and NLC findings. Tellurite glasses are a particularly noteworthy material that outperforms most other existing substances in the case of mechanical rigidity and optical durability. In addition, tellurite maintains a lower degree of toxicity when correlated to other forms of glasses and its nonlinear RI is 10 times greater than silica, making it a more environmentally-friendly choice. Further, operating this glass has a number of other notable benefits, involving an outstanding chemical permanence, digestion resistance, greater nonlinear RI coefficient and infinitesimal cut-

off phonon energies of around $600 - 800\ cm^{-1}$. Conclusively, an approximated temperature of $800°C - 900°C$ is capable of melting the tellurite glasses, which may subsequently be developed through the casting or ejection procedures [27, 55]. All of the above-alluded exciting traits have sparked a lot of interest and consideration. Therefore, the designed PCF has been employed using fused silica in the clad and tellurite in the core.

The primary focuses of this research investigation are to acquire highly nonlinear and birefringent responses, as well as negative-sloping dispersion, minimal confinement loss, higher effective mode area and numerical aperture, etc. Accordingly, a simple Hexa-circular core-based tellurite-filled PCF to fulfill these objectives. Especially, the simulated results delineate that the devised PCF consecutively depicts an ultra-high Br and NLC of 0.0924 and $18900\ W^{-1}Km^{-1}$, respectively at the popular optical wavelength of $1.55\ \mu m$. The practical implementation of the modeled fiber is anticipated to be feasible operating the existent fabrication procedures, as well as it can be suitable for pragmatic applications in numerous optical domains.

2. Design and Geometry

Due to its outstanding transparency and incredibly low loss behavior throughout the transmission spectrum, fused silica is operated in the clad of the devised PCF. Notably, it is considered an exciting material for long-distance optical communications. Tellurite glass, conversely, is operated in the core area because of the many advantages it possesses over other existing glasses. The developed PCF contains an asymmetrical core, contributing in the achievement of much higher birefringent, as well as other pertinent optical responses. The devised PCF is comprised of a pure Hexa-circular geometrical structure containing multiple circular air holes in its design. Pitch, designated as Λ, is expressed as the span between two neighboring circular slots estimated from the base of each slot. Λ is the only autonomous variable in the geometrical structure on which the other mathematical parameters wholly depend upon. The geometrical properties like air-hole diameters and pitches of modelled PCF have been varied using COMSOL Software. Keeping the fabrication tolerance in mind, having changed the values of the parameters and thus, achieved the desired results.

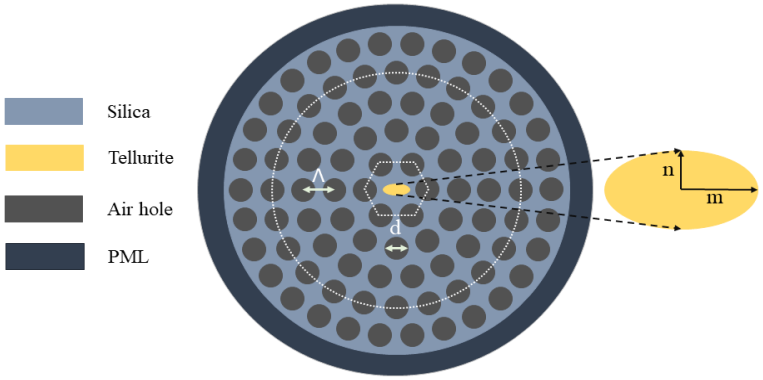

Fig. 1. Cross-sectional depiction of the Tellurite-filled Hexa-circular-timbered PCF.

The value of optimum pitch in the devised PCF is, $\Lambda = 0.80\ \mu m$. The estimated value of each diameter of the circular air holes is, $d = 0.90 \times \Lambda\ \mu m$. Notably, a tellurite-filled ellipse is inserted into the core area of the developed PCF, whose two prime semi axes (major and minor) are consecutively are $1 \times \Lambda$ and $0.5 \times \Lambda$. Further, a layer termed PML is inserted into the outside part of the fiber having a thickness equal to 10% of the overall PCF thickness.

3. Simulation Method and Discussion

A meticulous numerical breakdown is a must to scrupulously portray the devised PCF. As a consequence, the FEM is operated in conjunction with the COMSOL software to simulate the modal traits and geometrical parameters of the developed PCF. In terms of equational basis, Refs. [43] and [44] sequentially contain a thorough exploration of the RI of tellurite and silica glasses at ambient temperature, as well as the required observations and computations throughout a wide wavelength spectrum spanning the visible to microwave wavelength extents. The RI of fused silica and tellurite can be quantified by operating the Sellmeier expression [44, 43]. The mathematical statement is as follows [27]:

$$n(\lambda) = \sqrt{A + \frac{U_1\lambda^2}{\lambda^2 - V_1} + \frac{U_2\lambda^2}{\lambda^2 - V_2} + \frac{U_3\lambda^2}{\lambda^2 - V_3}} \quad . \tag{1}$$

Here, the exact value of A is 1 for both silica and tellurite glasses. Notably, U_1, U_2, U_3 and V_1, V_2, V_3 are Sellmeier coefficients whose actual values are accomplished from the Refs. [43] and [44] for tellurite and fused silica, successively. When it comes to fiber polarization states, birefringence (Br) is characterized as the dissimilarity in RI between two distinct polarization modes. The mathematical statement is as follows [45]:

$$Br = |n_x - n_y| \quad . \tag{2}$$

Here, n_x and n_y symbolize the effective RI of X and Y polarizations. The phrase effective mode area (EMA) can be operated to rigorously quantify the region covered by the mode fields within the core area. The mathematical statement to quantify EMA is as follows [46]:

$$A_{eff} = \frac{\left(\iint E^2 dxdy\right)^2}{\iint E^4 dxdy} \quad . \tag{3}$$

Here, the term E is portrayed as the amount of transverse electric field extending in the cross-section precinct of PCF. The nonlinear coefficients (NLC) of a PCF altogether rely upon the EMA and the nonlinear RI of the base substance. NLC of a fiber can be quantified by the ensuing mathematical statement [24]:

$$\gamma = \frac{2\pi}{\lambda} \times \frac{n_2}{A_{eff}}\ W^{-1}Km^{-1} \quad . \tag{4}$$

Here, the term n_2 conveys the nonlinear RI of tellurite, whose exact value is emanated from Ref. [43] and A_{eff} expresses the EMA of PCF as a function of the active wavelength. A further important metric associated with optical fiber transmission is dispersion, which is an amalgam of material and waveguide dispersions. The size and placements of the air holes in the clad have a mention-worthy impact on the dispersion behavior of a fiber. Notably, material dispersion holds an infinitesimal influence on total dispersion. Thus, total dispersion is roughly identical to waveguide dispersion, which can be quantified as follows [27]:

$$D(\lambda) = -\frac{\lambda}{c} \times \frac{d^2 R_e[n_{eff}]}{d\lambda^2} \ \ \mathrm{ps.nm^{-1}.km^{-1}} \quad . \tag{5}$$

where, $Re(n_{eff})$, λ and c consecutively symbolize the real segment of nonlinear RI, active wavelength and light speed in terms of a vacuum. An optical metric known as the numerical aperture (NA) expresses the range of angles through which light may be emitted in non-dimensional space. It can be estimated operating the ensuing mathematical formula [47]:

$$NA = \left(1 + \frac{\pi A_{eff}}{\lambda^2}\right)^{-\frac{1}{2}} \quad . \tag{6}$$

Conclusively, when developing a PCF, the confinement loss (CL) should be kept to a minimum extent since a higher CL can lessen the propagation length of the fiber [55]. CL can be quantified as follows [48]:

$$CL = 8.868 \times k_0 \times I_m[n_{eff}] \times 10^4 \ [dB/cm] \quad . \tag{7}$$

Here, $k_0 = \frac{2\pi}{\lambda}$; which is characterized as free-space wave-number.

The electric mode field distribution (MFD) of X and Y fundamental modes of the devised PCF are consecutively delineated in Figs. 2(a) and 2(b), which are rigidly inspected operating the COMSOL software.

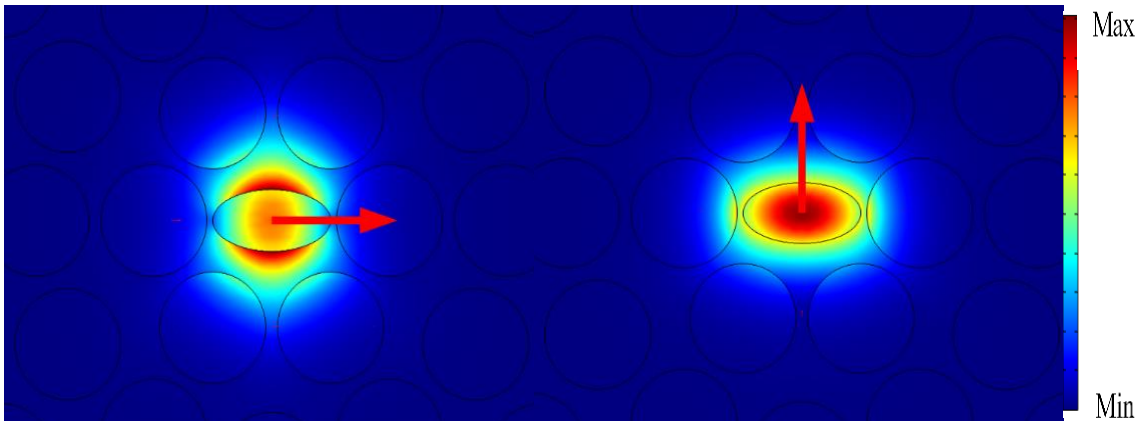

(a) *(b)*

Fig. 2. The MFD of (a) X and (b) Y at the active wavelength of 1.55 *μm.*

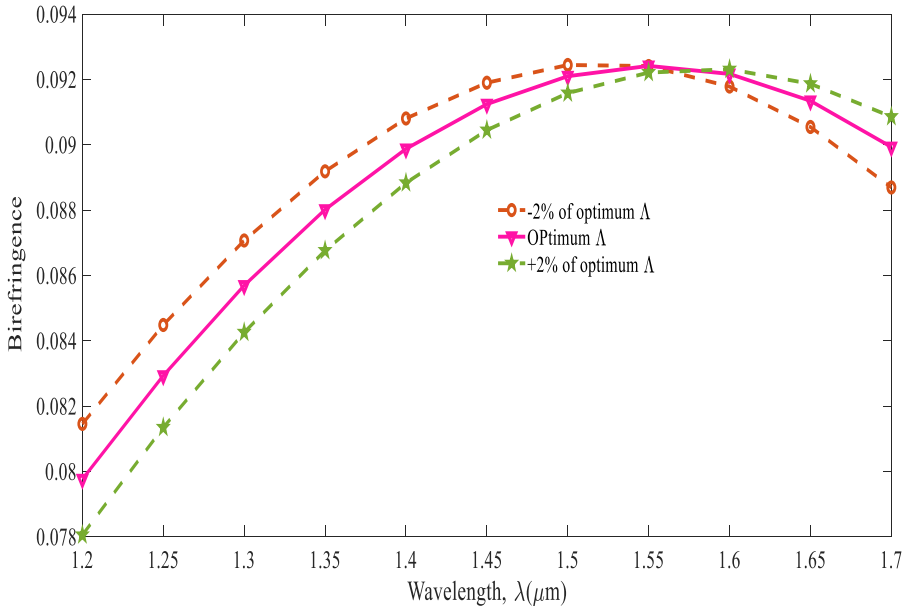

Fig. 3. Br vs. wavelength when the architectural parameters are optimized.

Fig. 3 delineates the behavior of Br as a function of wavelength with $\pm 2\%$ fabrication variation from the optimum design parameter pitch. A maximum Br of 0.0924 is noticed at the wavelength of 1.55 μm, where no changes of Br are found due to the alteration of optimum pitch. Particularly, it is observed that the Br is increasing with reference to wavelength before 1.55 μm wavelength. Afterward, the birefringent values gradually decrease. Optically birefringent fibers assist in reducing the PMD effect, as well as possess pragmatic utilization in polarization absorption and sensing purposes [27, 35]

The dispersion behavior with reference to wavelength is outlined in Fig.4, where a negative-sloping dispersion characteristic is notably perceived with the augmentation of wavelength. The dispersion characteristic of the devised fiber is markedly more negative for X-polarization than that of the Y-polarization. Besides, a near zero dispersion trait, ranging from 1.20 to 1.40 μm wavelengths, is obtained for Y-mode. Specifically, the dispersion of X and Y modes are -1665.25 and $-469.83\ ps.nm^{-1}.km^{-1}$ correspondingly, at 1.55 μm wavelength. It is prominent that the developed fiber achieves remarkably higher negative-sloping dispersion which plays a pivotal role in long-distance optical communication systems [27].

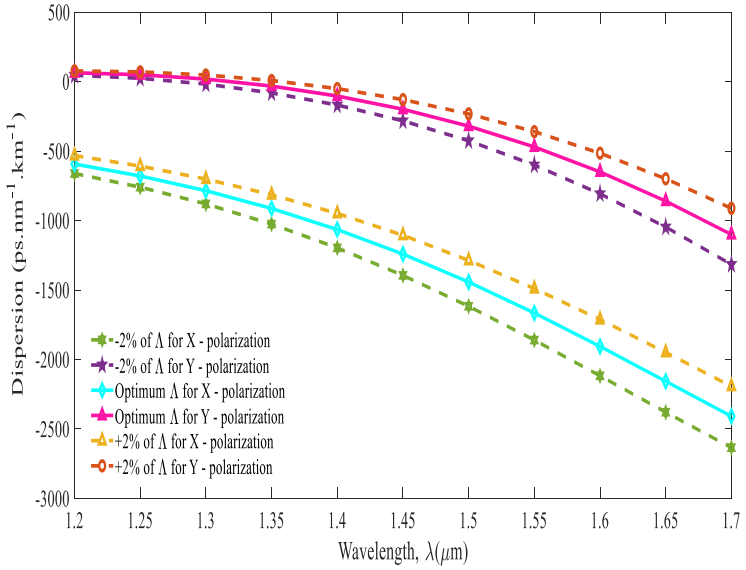

Fig. 4. Dispersion vs. wavelength when the architectural parameters are optimized.

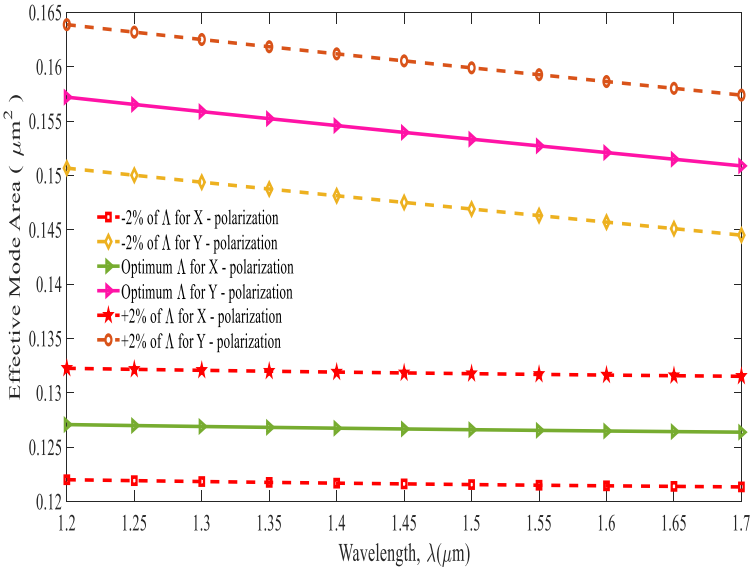

Fig. 5. EMA vs. wavelength when the architectural parameters are optimized.

Fig. 5 delineates the optical response of EMA as a function of wavelength for the optimal design parameter. It is palpable that the EMA of Y-mode is scarcely higher than the other mode. Specifically, an EMA of 0.126 and 0.1530 μm^2 is obtained at 1.55 μm wavelength for X and Y modes, successively. It is acknowledged that the PCF structures with large EMA trait can abolish most of the undesirable nonlinear effects. This particular optical attribute plays a paramount part in pertinent high-power purposes, namely high-power fiber sensors, amplifiers, lasers and so forth [49, 50].

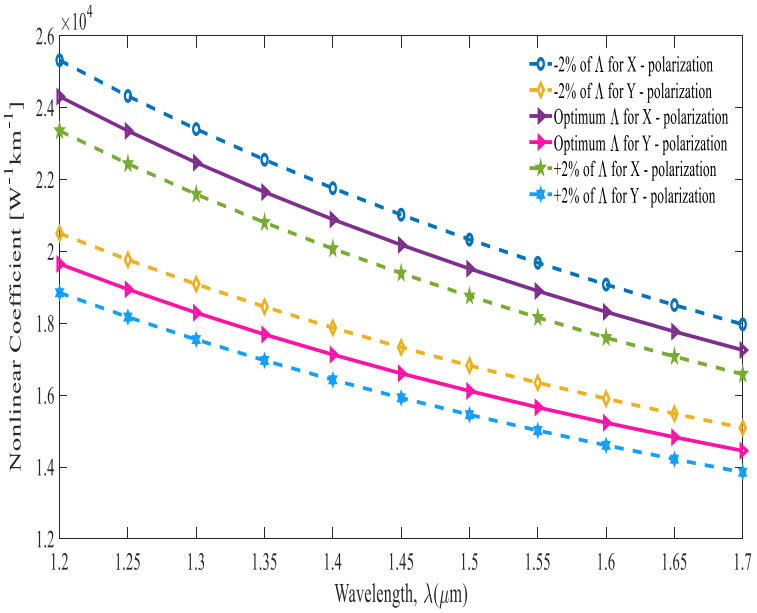

Fig. 6. NLC vs. wavelength when the architectural parameters are optimized.

The nonlinear behavior with regard to wavelength is outlined in Fig. 6, where it is discernible that the NLC is decreasing with the enlargement of wavelength. Specifically, the NLC of X and Y modes are 18900 and 15660 $W^{-1}Km^{-1}$ successively, at 1.55 μm wavelength. Highly nonlinear optical fibers have a paramount part to play in generating supercontinuum, in addition to the myriad other pertinent and fitting objectives that they are capable of executing via their inherent properties. When PCFs with highly nonlinear coefficients are operated concurrently, it is quite conceivable that a decent number of large supercontinuum spectra will be generated in a rather small length of fiber [35]. Accordingly, the devised PCF will be suitable for a wide range of applications needing ultra-high nonlinearity, as depicted in this study.

Fig. 7 delineates the optical response of NA as a function of wavelength for the optimum design parameter. It is visible from the above illustration that the NA of X-mode is narrowly higher than that of the other polarization mode. Precisely, the NA for X and Y modes are 0.93 and 0.90 consecutively, at 1.55 μm wavelength. A wide NA is desired for optical broad sensing applications, which can be accomplished by increasing the RI deviation between the two regions (core and cladding) of a PCF [47]. Operating this devised geometrical structure with tellurite as the base material and fused silica in the clad which boosts the NA in the developed PCF.

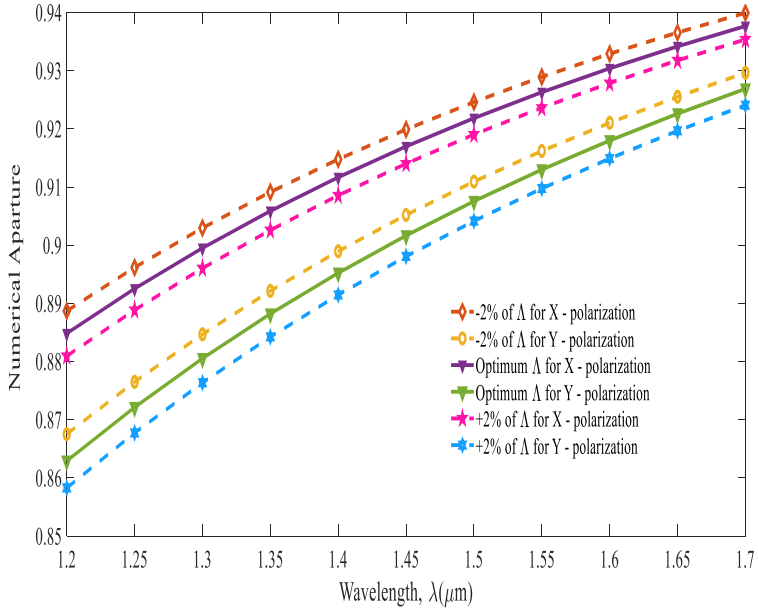

Fig. 7: NA vs. wavelength when the architectural parameters are optimized.

The behavior of CL curve with reference to wavelength is outlined in Fig. 8. In a PCF, the CL largely depends upon the number of air holes. The greater number of air holes assist in acquiring lower CL, which is decisive in designing an efficient fiber [39]. Notably, on an average, a minimal CL in the order of $10^{-10}\ dB/cm$ is observed in this devised PCF, which is a worthwhile part of this research inspection. Moreover, it is perceived that the obtained outcomes remain almost unchanged as a consequence of the parameter alteration, indicating that the developed PCF will operate as expectedly even if fabricated in practice.

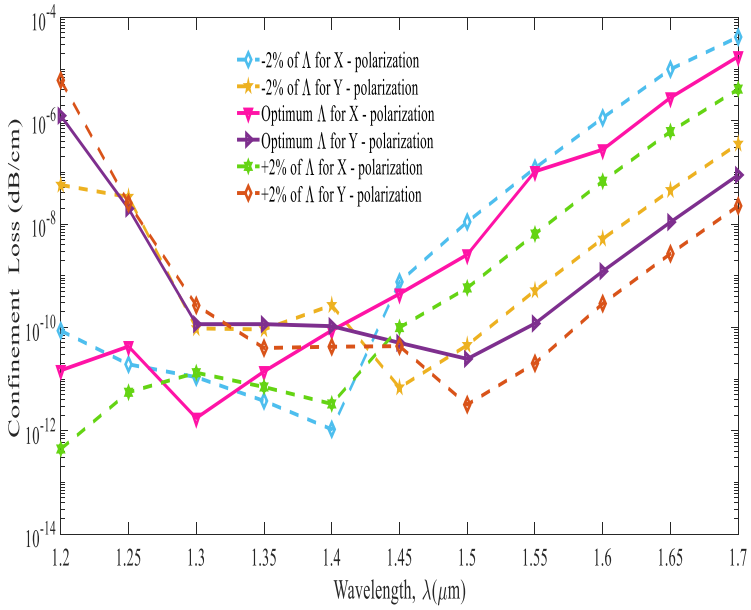

Fig. 8. CL vs. wavelength when the architectural parameters are optimized.

Table 1. A comparative analysis of the devised design with other prior PCF structures.

Reference	Nonlinearity, $W^{-1}Km^{-1}$	Birefringence	Wavelength
Ref [24]	1896	5.05×10^{-2}	$1550\ nm$
Ref [25]	188.39	7.57×10^{-2}	$1550\ nm$
Ref [26]	74.68	–	$1550\ nm$
Ref [27]	7333	5.85×10^{-2}	$1550\ nm$
Ref [28]	23.46	2.2×10^{-3}	$1550\ nm$
Proposed	18900	9.24×10^{-2}	$1550\ nm$

Conclusively, Table-1 delineates an in-depth comparative analysis between the previously documented designs with the devised PCF architecture. Here, it is obvious that the modeled design outperforms most of the existent PCF structures in terms of a considerable amount of relevant optical features, namely higher nonlinear and birefringent outcomes. Besides, it exhibits relatively minimal CL and higher EMA, as well as negative-sloping dispersion characteristics, which are seminal for pertinent optical applications.

4. Fabrication feasibility

Fabrication feasibility is a crucial aspect to consider in terms of designing a fiber on which the practical applicability of a PCF entirely relies. A variety of traditional and advanced fabrication processes are currently available for practically devising a wide spectrum of fiber structures. The most prevalent such existing methods especially include stack and drilling, 3D printing, sol-gel, extrusion, capillary stacking, etc. Recently, Jabin et al. practically manufactured an intricated amoeba-faced irregular-structured PCF for biosensing purposes containing more than 10 ellipses [51]. Also, Islam et al. introduced a Zeonex-filled micro-structured hollow hexagonal-core PCF containing honeycomb air holes, which makes the structure extremely challenging. Regardless, they were also able to fabricate such a strenuous design in practice [54]. Additionally, Jiang et al. have shown the successful development of a ZBLAN-based PCF, consisting of a solid-core, high air-filling percentage and nanoscale characteristics utilizing the stack-and-draw technique, where all the air holes are of irregular shape [36]. Another illustration of practical fabrication is the micro-structured polymer PCF developed by Argyros and colleagues [52], which has circular-fashioned air holes and was devised in the laboratory applying the standard capillary stacking technique. Regardless, the lack of sufficient air holes throughout the manufacturing process may result in strain. Conclusively, Bise et al. [53] devised a sol-gel casting procedure that can be used to concoct PCFs of almost any structural form, with the air-hole layout, as well as the shape and dimensions and other geometrical parameters, being freely adjustable independently. As a consequence of using this technique which anticipates that the proposed PCF has more design flexibility for further practical consideration. From the above-alluded discussion, it is obvious that many researchers have practically fabricated a decent number of PCFs with multiple ellipses and complicated structures. Consequently, the proposed fiber comprised of a relatively simpler structure can also be practically fabricated in the laboratory, where the dimension of the designed PCF can be adjusted freely.

5. Conclusion

A relatively simple tellurite-filled hexa-circular-coated PCF having highly nonlinear and birefringent responses have been offered in this investigation. Other compelling features of the modeled PCF include significantly higher EMA, lower CL and negative-sloping dispersion traits. Numerical experimentations affirm a superior Br of 0.0924 and an ultra-high NLC of $18900\ W^{-1}Km^{-1}$ can be acquired for optimal geometrical parameters at the popular optical wavelength of $1.55\ \mu m$. Furthermore, the devised PCF is capable of being practically realized

utilizing the existing fabrication procedures. Conclusively, with such exceptional optical modal traits, the developed PCF is envisaged to open a plethora of new windows for future applications in a variety of pertinent disciplines of optics and photonics, including polarization retention in long-distance communications, optical switching, sensor and laser layout, supercontinuum generation for frequency metrology, etc.

References

[1] J. C. Knight, T. A. Birks, P. J. St Russell, D. M. Atkin, Optics Letters, vol. 21, no. 19, pp. 1547-1549, 1996; https://doi.org/10.1364/OL.21.001547.
[2] J. C. Knight and P. S. J. Russell, Science, vol. 296, no. 5566. pp. 276–277, Apr. 12, 2002; https://doi.org/10.1126/science.1070033
[3] P. Russell, Science, vol. 299, no. 5605, pp. 358-362, Jan. 17, 2003; https://doi.org/10.1126/science.1079280
[4] P. Russell, IEEE Leos Newsletter, vol.21, no. 10, pp. 1–5, 2007.
[5] F. Luan et al, Optics Express, vol. 12, no. 5, pp. 835–840, 2004; https://doi.org/10.1364/OPEX.12.000835
[6] S. Arismar Cerqueira, Reports on Progress in Physics, vol. 73, no. 2, 2010; https://doi.org/10.1088/0034-4885/73/2/024401
[7] X. Sang, P. L. Chu, and C. Yu, Optical and Quantum Electronics, vol. 37, no. 10. pp. 965–994, Aug. 2005; https://doi.org/10.1007/s11082-005-8338-4
[8] R. Buczynski, *Acta Physica Polonica Series A*, vol. 106, no. 2, pp. 141-168, 2004;
[9] T. A. Birks, J. C. Knight, and P. J. St Russell, Optics Letters, vol. 22, no. 13, pp. 961-963, 1997; https://doi.org/10.1364/OL.22.000961
[10] J.C. Knight, T.A. Birks, R.F. Cregan, P. S. J. Russell and J.-P. de Sandro, Electronics Letters, vol. 34, no. 13, pp. 1347–1348, 1998; https://doi.org/10.1049/el:19980965
[11] N. G. R. Broderick, T. M. Monro, P. J. Bennett, and D. J. Richardson, Optics Letters, vol. 24, pp. 1395-1397, 1999; https://doi.org/10.1364/OL.24.001395
[12] F. Poli, A. Cucinotta, S. Selleri, and A. H. Bouk, IEEE Photonics Technology Letters, vol. 16, no. 4, pp. 1065–1067, Apr. 2004; https://doi.org/10.1109/LPT.2004.824624
[13] V. Finazzi, T. M. Monro, and D. J. Richardson, IEEE Photonics Technology Letters, vol. 15, no. 9, pp. 1246–1248, Sep. 2003.
[14] J.C. Knight, *Nature*, vol. 424, pp. 847-851, Aug. 2003; https://doi.org/10.1038/nature01940
[15] T. P. Hansen *et al.*, IEEE Photonics Technology Letters, vol. 13, no. 6, pp. 588-590, 2001; https://doi.org/10.1109/68.924030
[16] A. Ortigosa-Blanch, A. Díez, M. Delgado-Pinar, J. L. Cruz, and M. v. Andrés, IEEE Photonics Technology Letters, vol. 16, no. 7, pp. 1667–1669, Jul. 2004; https://doi.org/10.1109/LPT.2004.828524
[17] J. C. Knight, J. Arriaga, T. A. Birks, A. Ortigosa-Blanch, W. J. Wadsworth and P. S. J. Russell, IEEE Photonics Technology Letters, vol. 12, no. 7, pp. 807-809, July 2000; https://doi.org/10.1109/68.853507
[18] H. Ademgil and S. Haxha, Sensors (Switzerland), vol. 15, no. 12, pp. 31833–31842, Dec. 2015; https://doi.org/10.3390/s151229891
[19] B. K. Paul, K. Ahmed, Ceramics International, vol. 45, no. 1, pp. 1215-1218, Jan. 2019 https://doi.org/10.1016/j.ceramint.2018.09.307
[20] T. Yang, E. Wang, H. Jiang, Z. Hu, K. Xie, Optics Express, vol. 23, no. 7, p. 8329, Apr. 2015; https://doi.org/10.1364/OE.23.008329
[21] W. J. Wadsworth, J. C. Knight, W. H. Reeves, P. S. J. Russell, and J. Arriaga, Electronics Letters, vol. 36, no. 17, pp. 1452–1454, Aug. 2000 https://doi.org/10.1049/el:20000942
[22] H. Dobb, K. Kalli, and D. J. Webb, Electronics Letters, vol. 40, no. 11, pp. 657–658, May 2004; https://doi.org/10.1049/el:20040433

[23] M. Tonouchi, Nature Photonics, vol. 1, pp. 97–105, 2007; https://doi.org/10.1038/nphoton.2007.3
[24] J. Wang, Applied Optics, vol. 60, no. 15, p. 4455, May 2021; https://doi.org/10.1364/AO.423029
[25] M. Liu, H. Yuan, P. Shum, C. Shao, H. Han, L. Chu, Applied Optics, vol. 57, no. 22, p. 6383, Aug. 2018; https://doi.org/10.1364/AO.57.006383
[26] B. K. Paul, K. Ahmed, M. Thillai Rani, K. P. Sai Pradeep, and F. A. Al-Zahrani, Alexandria Engineering Journal, vol. 61, no. 4, pp. 2799–2806, Apr. 2022; https://doi.org/10.1016/j.aej.2021.08.006
[27] R. Amin, M. E. Khan, L. F. Abdulrazak, F. A. Al-Zahrani, and K. Ahmed, Physica Scripta, vol. 96, no. 12, Dec. 2021; https://doi.org/10.1088/1402-4896/ac227c
[28] R. Amin et al., Alexandria Engineering Journal, vol. 61, no. 12, pp. 11139-11147, December 2022; https://doi.org/10.1016/j.aej.2022.04.047
[29] P. A. Agbemabiese and E. K. Akowuah, Journal of Optical Communications, 2020; https://doi.org/10.1038/s41598-020-77114-x
[30] R. Amin et al., Alexandria Engineering Journal, vol. 61, no. 12, pp. 12915-12923, December 2022; https://doi.org/10.1016/j.aej.2022.06.054
[31] K. Ahmed, B. K. Paul, M. A. Jabin, and B. Biswas, Ceramics International, vol. 45, no. 12, pp. 15343–15347, Aug. 2019; https://doi.org/10.1016/j.ceramint.2019.05.027
[32] K. Ahmed *et al.*, Materials Discovery, vol. 7, pp. 8–14, Mar. 2017; https://doi.org/10.1016/j.md.2017.05.002
[33] J. Wei, J. M. Murray, J. O. Barnes, D. M. Krein, P. G. Schunemann, and S. Guha, Optical Materials Express, vol. 8, no. 2, p. 485, Feb. 2018; https://doi.org/10.1364/CLEO_SI.2017.SW4M.3
[34] N. Mohammadd et al., Journal of Ovonic Research, vol. 18, no. 2, pp. 129 – 140, Mar. 2022; https://doi.org/10.15251/JOR.2022.182.129.
[35] R. Amin, L. F. Abdulrazak, N. Mohammadd, K. Ahmed, F. M. Bui, and S. M. Ibrahim, Ceramics International, vol. 48, no. 4, pp. 5617-5625, Feb. 2022; https://doi.org/10.1016/j.ceramint.2021.11.106
[36] X. Jiang *et al.*, Nature Photonics, vol. 9, no. 2, pp. 133–139, Feb. 2015; https://doi.org/10.1038/nphoton.2014.320
[37] M. M. Hassan, K. Ahmed, B. K. Paul, M. N. Hossain, and F. A. al Zahrani, Physica Scripta, vol. 96, no. 11, Nov. 2021; https://doi.org/10.1088/1402-4896/ac13e1
[38] Z. Hui, Y. Zhang, and A. H. Soliman, Ceramics International, vol. 44, no. 9, pp. 10383–10392, Jun. 2018; https://doi.org/10.1016/j.ceramint.2018.03.052
[39] M. R. Islam, M. Arif Hossain, S. I. Ali, J. Sultana, and M. Saiful Islam, Journal of Optical Communications, vol. 42, no. 4, pp. 619–626, Oct. 2021; https://doi.org/ 10.1515/joc-2018-0152
[40] M. S. Islam, M. R. Islam, and J. Rahman, *Int. J. Microw.* Opt. Technol., vol. 14, no. 1, pp. 62–69, Jan. 2019.
[41] M. R. Islam, A. N. M. Iftekher, F. A. Mou, M. M. Rahman, and M. I. H. Bhuiyan, Applied Physics A: Materials Science and Processing, vol. 127, no. 2, Feb. 2021; https://doi.org/10.1007/s00339-020-04261-3
[42] M. S. Islam et al, Optical Fiber Technology, vol. 34, pp. 6–11, Mar. 2017; https://doi.org/10.1016/j.yofte.2016.11.014
[43] M. Klimczak et al, Journal of the Optical Society of America B, vol. 36, no. 2, p. A112, Feb. 2019; https://doi.org/10.1364/JOSAB.36.00A112
[44] A. Upadhyay, S. Singh, D. Sharma, and S. A. Taya, Theoretical Insight," 2021; https://doi.org/10.21203/rs.3.rs-227813/v2
[45] J. Sultana *et al.*, Optics Communications, vol. 407, pp. 92–96, Jan. 2018; https://doi.org/10.1016/j.optcom.2017.09.020
[46] Md. S. Islam, J. Sultana, J. Atai, D. Abbott, S. Rana, and M. R. Islam, Applied Optics, vol. 56, no. 4, p. 1232, Feb. 2017; https://doi.org/10.1364/AO.56.001232

[47] M. S. Islam *et al*, IEEE Sensors Journal, vol. 18, no. 2, pp. 575–582, Jan. 2018; https://doi.org/10.1109/JSEN.2017.2775642
[48] S. Islam *et al.*, Optical Engineering, vol. 55, no. 7, p. 076117, Jul. 2016; https://doi.org/10.1364/JOSAB.34.001747
[49] A. Dutt, S. Mahapatra, and S. K. Varshney, Journal of the Optical Society of America B, vol. 28, no. 6, p. 1431, Jun. 2011; https://doi.org/10.1364/JOSAB.28.001431
[50] Reena, T. S. Saini, A. Kumar, Y. Kalra, and R. K. Sinha, Applied Optics, vol. 55, no. 15, p. 4095, May 2016; https://doi.org/10.1364/AO.55.004095
[51] M. A. Jabin et al, Sensors and Actuators, A: Physical, vol. 313, Oct. 2020; https://doi.org/10.1016/j.sna.2020.112204
[52] A. Argyros et al., Optics Express, vol. 9, no. 13, pp. 813-820, 2001; https://doi.org/10.1364/OE.9.000813
[53] R. T. Bise and D. J. Trevor, OFC/NFOEC Technical Digest. Optical Fiber Communication Conference, 2005; https://doi.org/ 10.1109/OFC.2005.192772
[54] S. R. Tahhan, H. K. Aljobouri, Journal of Optical Communications, 2020; https://doi.org/ 10.1109/OFC.2005.192772
[55] Md. S. Islam *et al*, Advanced Photonics Research, vol. 2, no. 12, p. 2100165, Dec. 2021; https://doi.org/10.1002/adpr.202100165
[56] R. Amin et al., Physica Scripta, 2022; https://doi.org/10.1088/1402-4896/ac5359